inorganics

MDPI

Article

Effect of CaO-TiO_2-SiO_2 on the Microstructure and Mechanical Properties of Ceramic Corundum Abrasives

Quanbao Zhao, Zhihong Li and Yumei Zhu *

Key Laboratory for Advanced Ceramics and Machining Technology of Ministry of Education, School of Materials Science and Engineering, Tianjin University, Tianjin 300072, China
* Correspondence: tjuzhuyumei@163.com

Abstract: Ceramic corundum abrasives were prepared using pseudo-boehmite as a raw material via the sol-gel method. Additives can significantly change the microscopic morphology of abrasives and improve mechanical properties. When 2 wt% CaO-TiO_2-SiO_2 with a molar ratio of 3:4:9 was added, samples with the best morphology and mechanical properties were obtained. Single-particle compressive strength, density, Vickers hardness, and average grain size were 51.45 N, 3.94 g·cm^{-3}, 16.43 GPa, and 0.98 µm, respectively. We compared the same additive system with abrasives prepared by ball milling, and found that ball milling was beneficial for obtaining denser and smaller grain size abrasives. On the other hand, abrasives obtained without ball milling had relatively higher single-particle compressive strength. Additionally, the additives are non-precious metal oxides, which can reduce the cost of the synthesis process. In addition, there has been discussion of the connection between microstructure and mechanical characteristics.

Keywords: ceramic corundum; sol-gel process; additives; strength

Citation: Zhao, Q.; Li, Z.; Zhu, Y. Effect of CaO-TiO_2-SiO_2 on the Microstructure and Mechanical Properties of Ceramic Corundum Abrasives. *Inorganics* **2023**, *11*, 187. https://doi.org/10.3390/inorganics11050187

Academic Editor: Kenneth J.D. MacKenzie

Received: 2 April 2023
Revised: 19 April 2023
Accepted: 21 April 2023
Published: 26 April 2023

1. Introduction

Ceramic corundum abrasives have smaller grain size and higher mechanical properties such as hardness, toughness, self-sharpening, wear resistance, and smaller grain size compared to traditional fused corundum abrasives. Moreover, their cost is lower than that of superhard abrasives, namely diamond and cBN [1–3]. These abrasives fill the gap between traditional fused corundum abrasives and superhard abrasives in terms of price and performance, and therefore have broad application prospects in the field of grinding [4–6]. To accelerate the grain growth and densification process, additives and seeds are typically added to these abrasives. These substances affect the microscopic morphology and improve the mechanical properties of abrasives. Thus, by controlling the introduction of additive substances, the controllability of abrasives can be achieved to a certain extent [7–9].

The main component of ceramic corundum abrasives is α-Al_2O_3, which is the most stable phase among all the phases of alumina. All other crystalline alumina will be converted into α-Al_2O_3 above 1200 °C. The α-phase transition is the phase transition of lattice reconstruction, and the process of nucleation and growth occurs at the same time [10–12]. Seeds provide more nucleation sites for grain growth, thus facilitating the sintering process and affecting the morphology and properties of the samples [13–15]. The addition of seeds can also promote sintering compaction and reduce the grain size. Additives play an important role in the sintering process. The bond energy between the Al and O of Al_2O_3 is very high. Although the phase change temperature is above 1100 °C, compaction requires a temperature above 1600 °C. On one hand, high temperature not only increases energy consumption and production cost, but also has high requirements on production equipment; on the other hand, high temperature frequently results in irregular grain development or recrystallization, which impairs the effectiveness of ceramic corundum abrasives. Due to the introduction of additives, the sintering temperature or phase transition temperature

is lowered, and the grain boundary structure is changed, affecting the microstructure of ceramics [16,17]. The mechanism of action between additives and alumina can be divided into the following three types: forming a solid solution, forming a low-temperature liquid phase, and forming an intermediate or second phase [18]. For instance, SiO_2 can form a low-temperature liquid phase with alumina and other metal oxides, thereby promoting the sintering of Al_2O_3 ceramics [19,20]. TiO_2 can create a limited solid solution with Al_2O_3, increasing lattice defects, allowing the activation energy of sintering, and promoting the sintering of Al_2O_3. The introduction of TiO_2 accelerates the sintering process of Al_2O_3 ceramics and significantly reduces the sintering temperature. As long as the added amount is appropriate, the impact on the performance is small, which has practical significance in the production. However, the content of additives should be controlled within an appropriate range. Otherwise, the excess additives will accumulate at the grain boundaries, and abnormal grain growth (AGG) will happen when the content exceeds the solubility limit. Park and Yoon [21] found AGG when adding 100 ppm of SiO_2 and 50 ppm of CaO.

Moreover, ball milling is an effective mechanical activation method that can reduce alumina's alpha transformation temperature. During the ball milling process, grain refinement, phase transformation, and the creation of internal defects occur [22]. The strain energy in the powder particles is effectively released during the ball milling process, reducing the activation energy of the phase transition and thereby lowering the phase transition temperature. Additionally, the powder produces mass nuclei during ball milling, which increases the nucleation density. Furthermore, ball milling allows for more uniform mixing of raw materials, seeds, and additives. Thus, it is widely used to prepare ceramic corundum abrasives, although it may limit preparation efficiency in some cases.

Previous research has yielded outstanding results but overlooked the quantity requirements for actual production. Due to the difference between the actual production and laboratory preparation processes, the abrasives' performance obtained by the same system will vary greatly. Therefore, we used the mixing method to introduce additives to simulate the actual production mixing method and solve the problem of relatively lower production efficiency. The synergistic effect of the adopted additive systems dramatically improves the abrasive performance and outperforms the effect of unitary and binary additive systems. Moreover, the chosen additives are safe and pollution-free, and their price is relatively lower. CaO can develop a liquid phase with the Al_2O_3 matrix or form a low-temperature liquid phase under the combined action of SiO_2 or TiO_2, promoting the sintering of alumina ceramics [23]. In this work, we analyzed the effects of different contents of the CaO-TiO_2-SiO_2 system on the morphology and properties of the prepared ceramic corundum abrasive, while keeping the molar ratio of TiO_2 and SiO_2 constant. We also analyzed the relationship between abrasive morphology and mechanical properties. Our findings aim to provide a reference for production in practical quantities.

2. Results and Discussions

SEM micrographs of S0–S5 are shown in Figure 1. As shown in Figure 1a, in the absence of additives (sample S0), the thermal energy alone may not be sufficient to promote complete grain growth. Incomplete growth of the grains results in numerous stomata between the grains, which weakens the properties of ceramic corundum abrasives.

Figure 1b–f shows that the addition of additives can significantly promote grain growth and affect the morphology. CaO acts together with SiO_2 and TiO_2 to form a low-temperature liquid phase that can promote sintering when the addition amount is low. However, exceeding a limit concentration will lead to AGG [24]. When the content of CaO is low, the growth promotion effect of SiO_2 and TiO_2 is more apparent, and the abrasive shows a rod-like and flake-like complex structure (Figure 1b–d). When the content of SiO_2 is too high, the grains are slender and needle-like/rod-like. The joint action of SiO_2 and CaO causes AGG, while the solo addition of CaO will not cause AGG. With the increase of CaO content, the anisotropy of the abrasives decreases, showing a trend of equiaxed grains (Figure 1e). However, the grains grow abnormally when CaO is excessive, which is

caused by the accumulation of excess additives at the grain boundaries (Figure 1f). Hong et al. [25] found that anisotropic grain growth only occurs in a relatively limited range of liquid phase content. Altay and Mehmet [26] also observed that when excessive amounts of calcium impurities at the grain boundaries reached a threshold level, this resulted in elongated grain morphology.

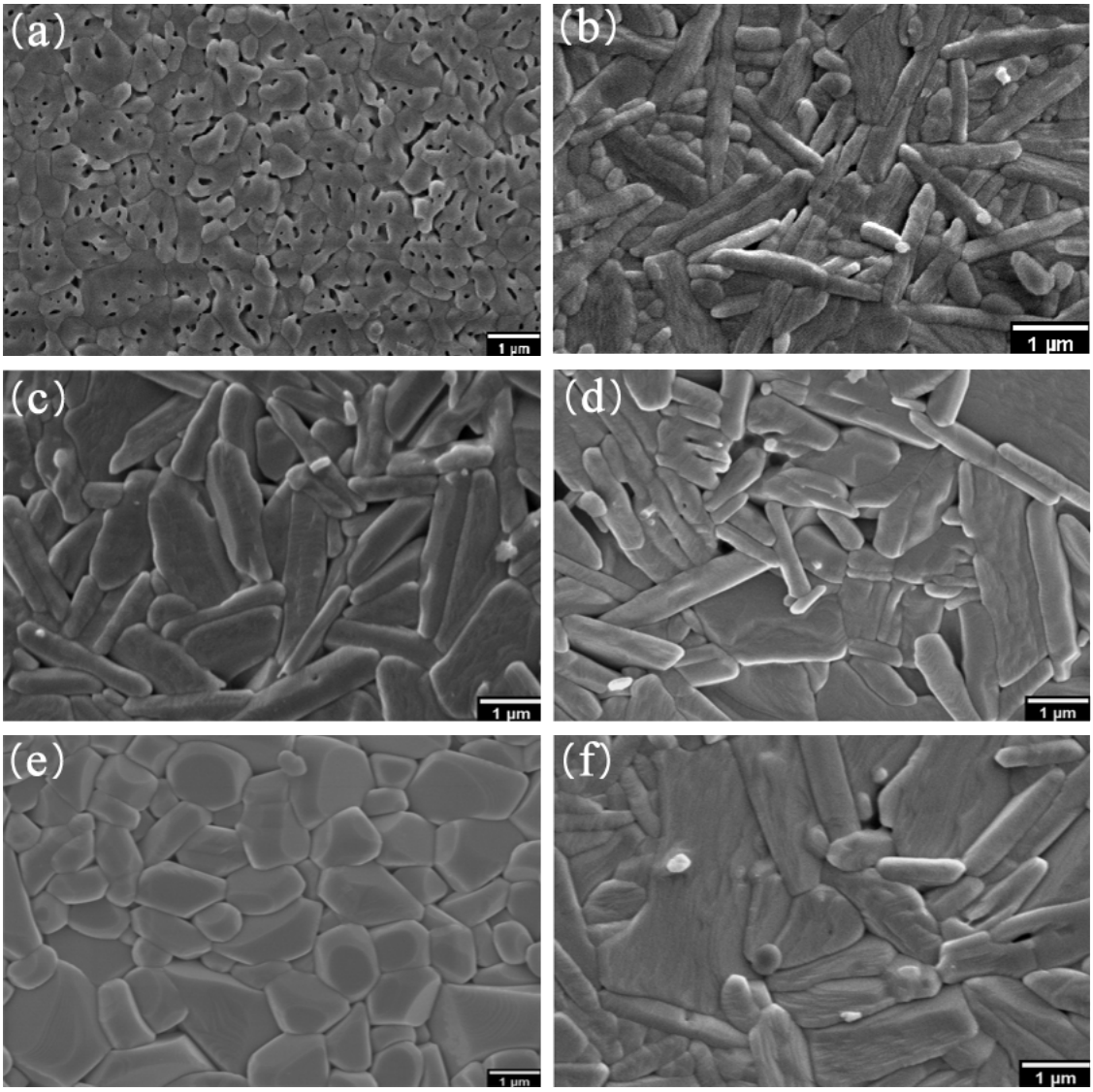

Figure 1. SEM micrographs of the samples with different molar ratio additives: (**a**) S0; (**b**) S1; (**c**) S2; (**d**) S3; (**e**) S4; (**f**) S5.

When the amount of liquid phase formed is too large, a large number of grains grow rapidly at the same time. Therefore, grains collide and stop growing. Overall, it is more difficult for anisotropic grain growth when the liquid content is higher, and the grains of Al_2O_3 tend to grow normally. This shows that when the molar ratio of CaO, SiO_2, and TiO_2 is 3:4:9, more liquid phases are formed during the sintering process, which can ensure that the grains grow normally (Figure 1e). On the other hand, SiO_2 forms a glass phase during the sintering process, which affects the viscosity of the liquid phase. When its content is too high, the liquid phase viscosity will increase, hindering the densification process. The addition of TiO_2 weakens the strength of the glass network structure, assists crystallization in the glass phase, and decreases the viscosity [27]. However, high liquid phase viscosity is not conducive to the liquid phase mass transfer process, which can also lead to reduced compactness. The increase in CaO content reduces the liquid phase viscosity

and promotes liquid phase mass transfer. The additives promote the sintering process by a synergistic effect.

Because the molar ratio of TiO_2/SiO_2 is constant, and to facilitate the calculation, the ratio of CaO/TiO_2 was used as a variable to explore property changes. Figure 2 shows the single-particle compressive strength, density, and Vickers hardness of ceramic corundum abrasives as a function of CaO/TiO_2. The results show that with the increase of calcium oxide content, the compressive strength of single particles increases first and then decreases, which is consistent with the changes in density (Figure 2b,c). This is mainly because the grains inside the abrasive gradually change from needle/flake with lower strength to massive grain with higher strength. Compared with Figure 1c, grains in Figure 1b have better consistency, making them more tightly bound with fewer pores, resulting in higher density. When CaO is added, a small number of flake grains appear, resulting in some pores, causing the density to decrease. Due to the combination of lamellar and other grains, some pores are excluded. The density reaches its maximum when pores are almost eliminated (Figure 1e). On the other hand, the grain size in Figure 1e is smaller, resulting in a higher single-particle compressive strength of up to 51.45 N, and the density is 3.94 $g \cdot cm^{-3}$. Excessive CaO results in AGG and a lamellar structure, so the density decreases again, consistent with the microstructure features exhibited in Figure 1. The compactness of abrasives is reduced due to the existence of pores, making them easily fractured from these pores when subjected to external pressure. Therefore, there is a close relationship between single-particle compressive strength and density. As for Vickers hardness, it continues to increase until it stabilizes at a certain extent of about 16.75 GPa (Figure 2c). Compared with the sample without additives (S0), the Vickers hardness of samples increased by about 100%, significantly improving the mechanical properties. The density, single-particle compressive strength, and Vickers hardness of S2, S3, and S4 show the same trend, indicating that Vickers hardness is affected by additives and microstructure. The change in ball milling toughness is shown in Figure 2d. When the additive content changes, the ball milling toughness change curve of S1–S4 is similar to its density and single-particle compressive strength, while the change curve of S2–S5 is similar to its Vickers hardness, indicating that ball milling toughness is affected by multiple factors such as grain size and density. We obtained abrasives with higher strength and density than some previous studies. You et al. [28] reported that with the inclusion of the ternary compound additive Na_3AlF_6-CaO-SiO_2, corundum abrasives were created in a two-step sintering process with plate-like grains; however, the single-particle compressive strength was 49 N. Hu et al. [29] also investigated the synergistic effect of ZnF_2-TiO_2-SiO_2 and seeds on the sintering behavior and microstructure of corundum abrasives. By contrast, we prepared abrasives with higher strength by adding fewer additives. Reducing the cost and improving performance are of great significance in the actual production, and could significantly improve the preparation efficiency of ceramic corundum abrasives.

Figure 3 shows XRD diffraction result of S1-S5. It's confirmed that the main component of the samples is corundum. It can be a preliminary illustration that homogeneous ceramic corundum abrasives were obtained by combining Figure 1.

Figure 4 shows SEM micrographs and element distribution of the S4 sample. The grain composition and structure are homogeneous, and there is no second phase. Ca, Ti, and Si are evenly distributed on the surface of the grain to form a thin film. The thin film can inhibit the growth of the grain and prevent the initiation and expansion of microcracks, reduce the stress concentration inside the abrasive, and thus improve the strength of abrasives.

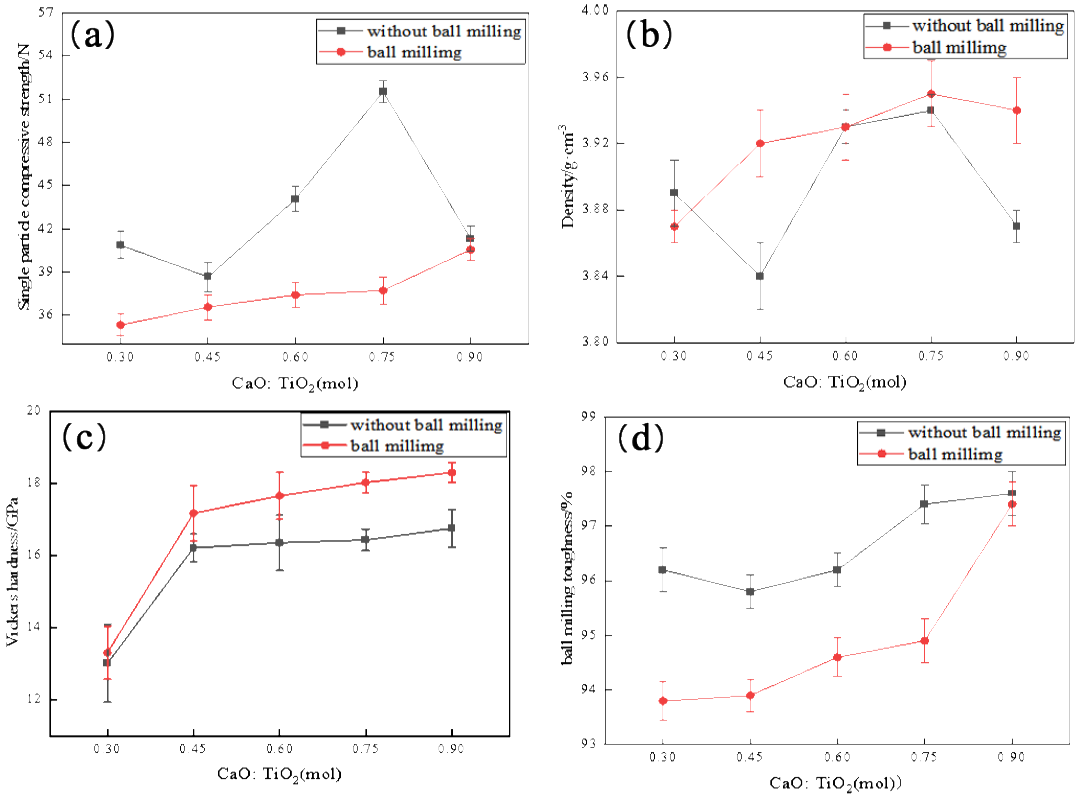

Figure 2. Mechanical properties of the samples with different molar ratio additives: (**a**) single particle compressive strength; (**b**) density; (**c**) Vickers hardness; (**d**) ball milling toughness.

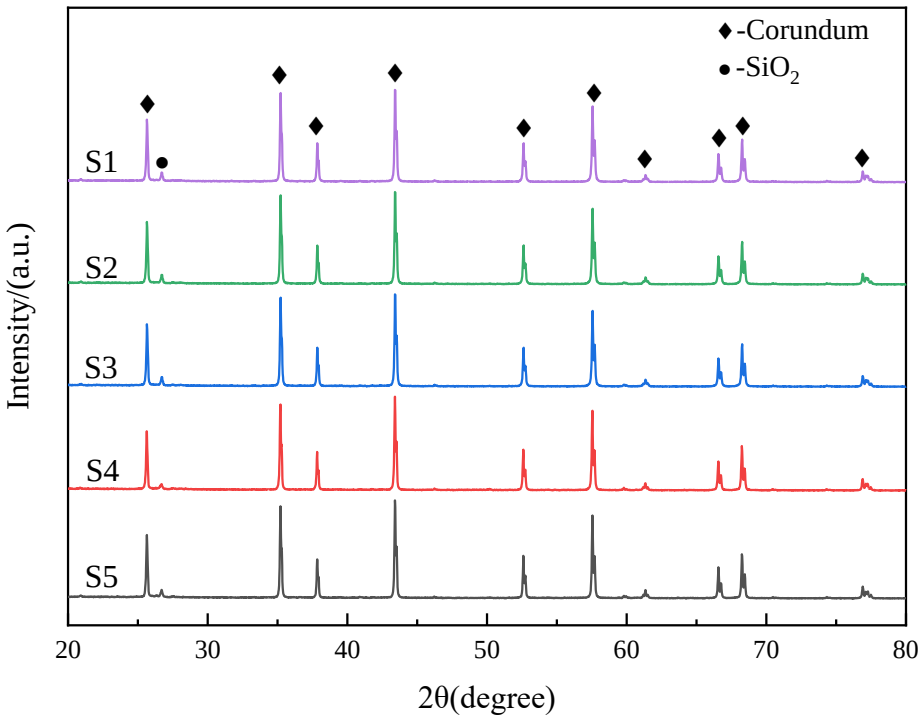

Figure 3. XRD diffraction result of S0-S5.

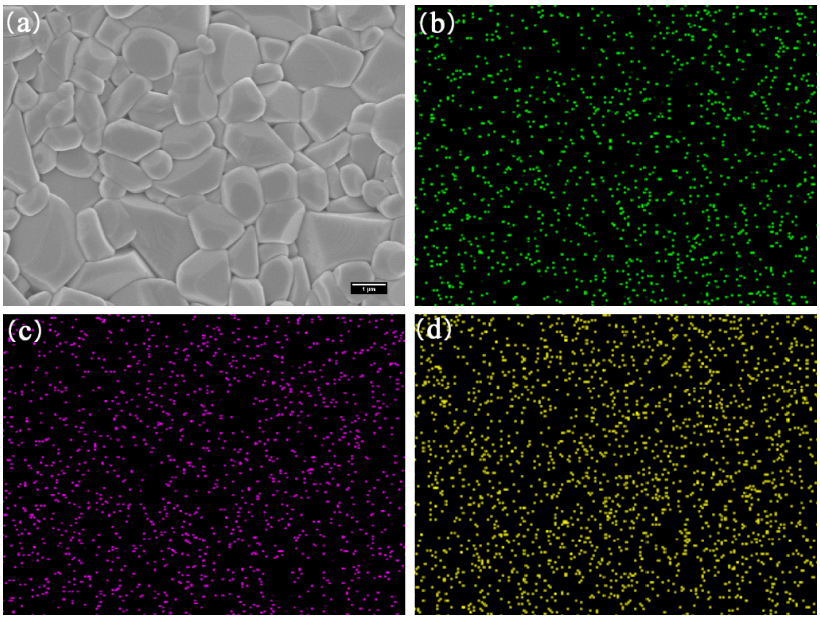

Figure 4. SEM micrographs and element distribution of S4 sample. (**a**) Microstructure; (**b**) Ca; (**c**) Ti; (**d**) Si.

To investigate the influence of the introduction method of the additives on the microstructure and mechanical properties of abrasives, samples with the same additives were prepared using ball milling (M1 to M5, as shown in Figure 5). The mechanical properties of M1 to M5 increase continuously as the ratio of CaO/TiO_2 increases, in contrast to S1 to S5 (Figure 2). Ball milling results in smaller abrasive grain sizes. The highest density, Vickers hardness, and single-particle compressive strength are 3.95 $g{\cdot}cm^{-3}$, 18.30 GPa, and 40.55 N, respectively. For example, when comparing S4 to M4, it is evident that M4 has finer grains and a more uniform distribution of grain sizes (Figure 6). The grain size distribution of M4 is mainly between 0.4 μm and 0.8 μm, and it has approximately normal distribution. In contrast, S4's grain size distribution is primarily between 0.4 μm and 1.4 μm, with an average grain size of 0.98 μm. Abrasives fabricated through ball milling exhibit higher density and Vickers hardness, while those fabricated through stirring have higher single-particle compressive strength. Generally, finer grains have better mechanical properties due to their smaller size and better compactness, resulting in higher density and Vickers hardness (Figure 2b,c). However, fracture occurs during single-particle compressive strength testing. The fracture surface and the partially enlarged view of abrasives are shown in Figure 7a,b, respectively. Figure 7a depicts a rough fracture surface, indicating toughness fracture, and Figure 7b shows the intergranular fracture of small-size grains and the transgranular fracture of large-size grains, which work together to improve ball milling toughness and safety during the grinding process. With a larger grain size, transgranular fracture occurs during fracture, while intergranular fracture occurs when the grain is smaller, thus absorbing less energy. Therefore, abrasives with larger grain sizes possess higher single-particle compressive strength and ball milling toughness in some cases. However, the safety problems caused by crystal fracture should be paid attention to, and grinding tools should be checked regularly. Microcracks, transgranular fractures, and intergranular fractures improve the strength by joint effect. It can also be concluded that samples obtained from the same additive system will be affected by the process. The preparation process can be chosen depending on practical use. The change in the Vickers hardness follows a different pattern than that of compressive strength and density in Figure 1, but it is consistent with Figure 5. It is worth noting that when the molar ratio of $CaO\text{-}TiO_2\text{-}SiO_2$ is 3:4:9, the microstructure and mechanical properties of ceramic corundum abrasives could achieve good results with whatever method of additive system is adopted,

which indicates that the effect of the additives is more obvious and can play a good role when the introduction mode is changed.

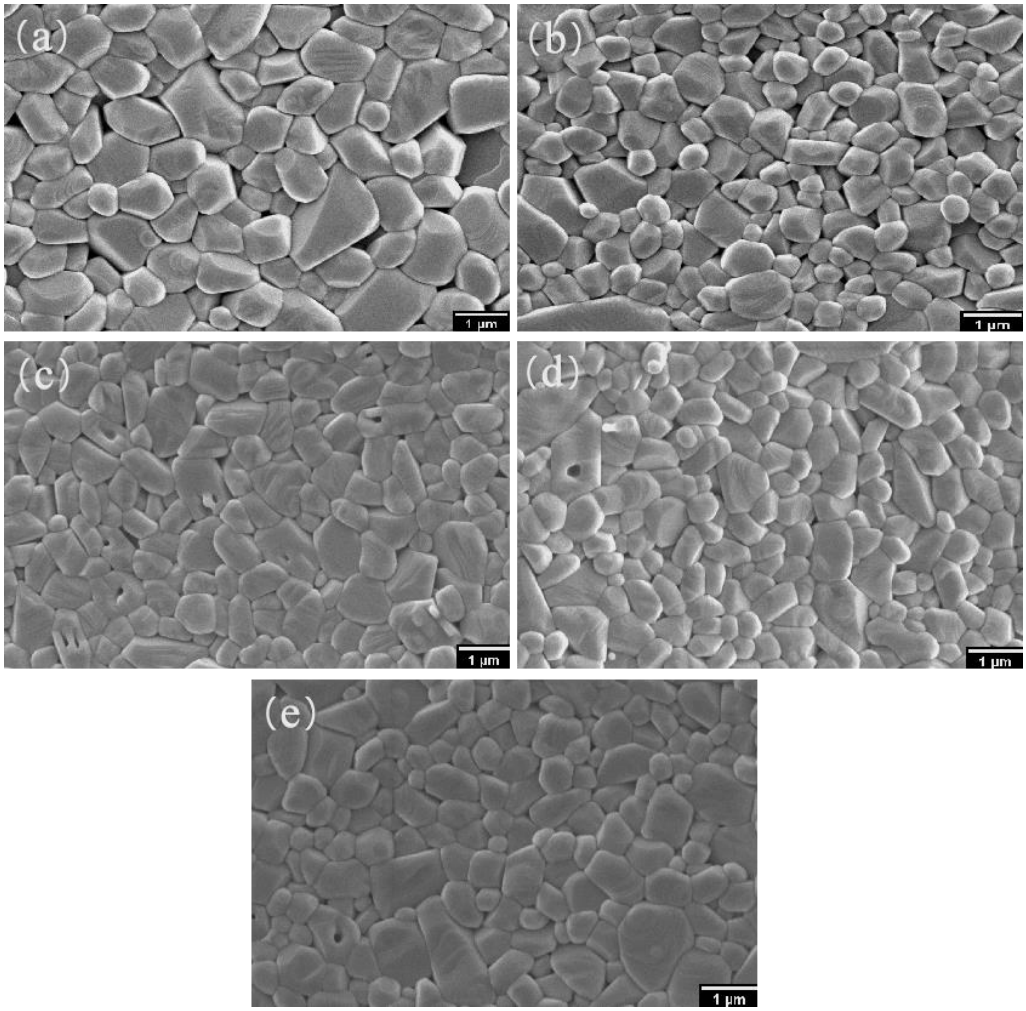

Figure 5. SEM micrographs of the samples with different molar ratio additives by ball milling: (**a**) M1; (**b**) M2; (**c**) M3; (**d**) M4; (**e**) M5.

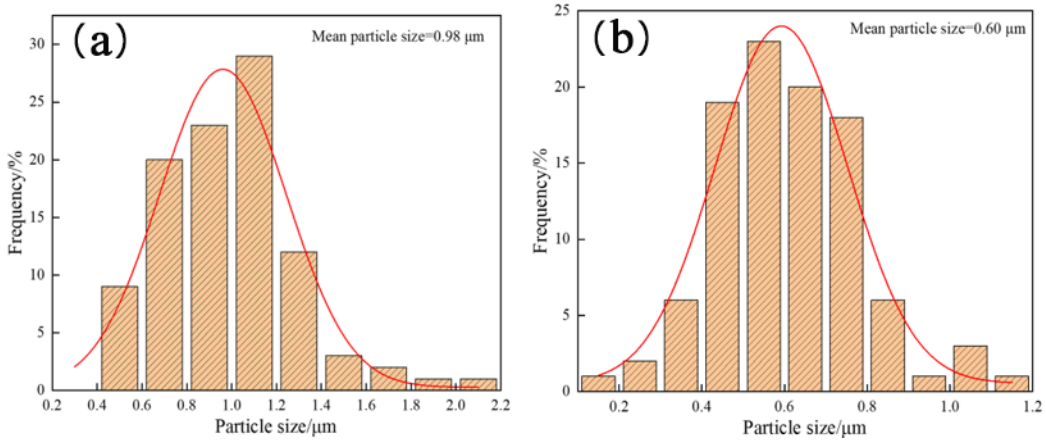

Figure 6. Particle size distributions by different ways of additive introduction: (**a**) S4;(**b**) M4.

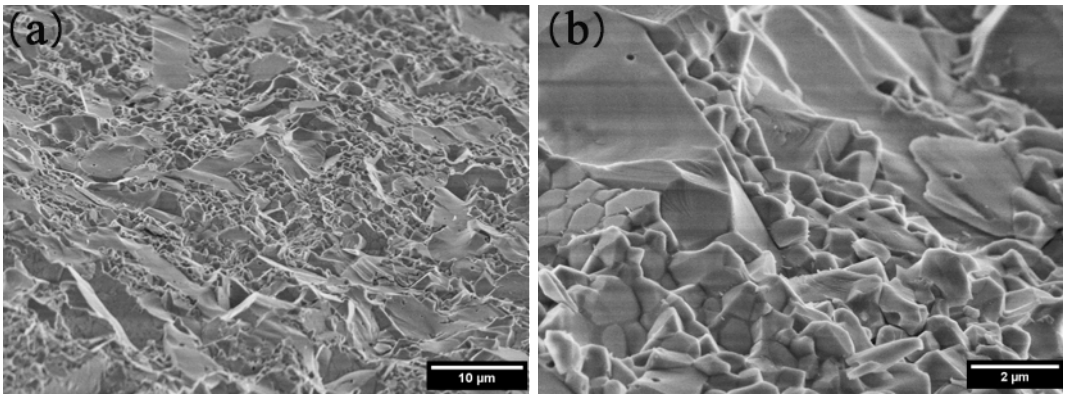

Figure 7. SEM micrograph of fracture surface and partially enlarged view of S4: (**a**) fracture surface; (**b**) partially enlarged view.

When choosing additives, the price and stability are also factors worth considering. Although some precious metal oxides can effectively promote or inhibit the growth of grains, the high cost is not conducive to industrial mass production, which limits the application of ceramic corundum abrasive. It also requires that additives are easy to store and transport, and their physical and chemical properties are stable to ensure the accurate content of metal ions introduced. The additives used in this paper can meet the above requirements well, and can reduce the production cost while promoting sintering by producing a liquid phase. SiO_2 is a cheap and common oxide; the formation of bonding in sintering plays an important role relative to improving the density of abrasives. Although the selected CaO may have the problem of water absorption in storage, choosing $CaCO_3$ as the introduced substance of Ca^{2+} could solve this problem. Both TiO_2 and SiO_2 are additives that obviously promote the growth of ceramic corundum abrasive grains, and they could effectively improve the microscopic density of the abrasives when added alone. Through complementary advantages, the three additives can produce ceramic corundum abrasives with dense structure and excellent performance at a low level of addition content.

3. Experimental Method

3.1. Sample Preparation

In this study, ceramic corundum abrasives were prepared via the sol-gel method, using pseudo-boehmite as the raw material. The solid content was 25%, and the seed crystal was α-Al_2O_3 prepared at 1200 °C. The additive system comprised CaO-TiO_2-SiO_2, with CaO and SiO_2 added in the form of $CaCO_3$ (AnalaR grade; Tianjin Bodi, Tianjin, China) and $(C_2H_5O)_4Si$ (TEOS, AnalaR grade; Kewei Ltd, Tianjin, China.), respectively. The specific experimental procedure was as follows: firstly, citric acid ($C_6H_8O_7$) was dissolved in water and stirred until completely dissolved and until the pH was approximately 3. Then, the pseudo-boehmite, 3 wt% seed crystal, and additives were mixed uniformly by stirring for 2 h. After that, the obtained sol was allowed to stand at room temperature for 1 h and was dried in an oven at 80 °C for 24 h. The dry gel was crushed and sieved to obtain 30-mesh to 40-mesh particles. The particles were then heated from room temperature to 1400 °C at a heating rate of 7 °C·min^{-1}, sintered, and kept for 1 h. Ceramic corundum abrasives without ball milling were obtained. The total amount of additives was 2 wt%, and the samples obtained in different proportions were labeled S0 to S5, as shown in Table 1. In addition, abrasives were obtained by ball milling to mix additives and raw materials and were labeled M1 to M5.

Table 1. Description and mechanical parameters of different samples.

Designation of Sintered Sample	Molar Ratio of CaO, TiO_2, and SiO_2	Single-Particle Compressive Strength/N	Vickers Hardness/GPa
S0	no adding	36.50	6.93 ± 0.30
S1	1.2:4:9	40.85	13.01 ± 1.08
S2	1.8:4:9	38.65	16.21 ± 0.38
S3	2.4:4:9	44.05	16.35 ± 0.77
S4	3.0:4:9	51.45	16.43 ± 0.30
S5	3.6:4:9	41.30	16.75 ± 0.53

3.2. Sample Characterization

A cold-field-emission scanning electron microscope (SEM, Hitachi-S4800,Hitachi, Tianjin, China) was used to analyze the microstructure of the morphology, distribution, and size of the grains. An EDS spectrum analyzes the element distribution at grain surfaces and grain boundaries by line scanning and surface scanning.

The density of abrasives was measured by the Archimedes drainage method. Before measuring the density, the particles of abrasives were dried at 110 °C to a constant weight, and cooled to room temperature in a desiccator. Abrasive particles were weighed, and their mass was recorded as m (the measured abrasive is generally not less than 1/3 of the volume of the pycnometer, and not more than 1/2). To measure the mass, the abrasives were poured into the pycnometer to vacuumize for 5 min. Next, distilled water was infused to immerse the abrasives, and vacuumization was continued for another 15 min. The pycnometer was then filled with distilled water, and the mass of the pycnometer filled with abrasives and distilled water was recorded as m_2. Finally, the abrasives and distilled water in the pycnometer were poured out, and the pycnometer was cleaned and refilled with distilled water. The mass of the pycnometer filled with distilled water was recorded as m_1. The formula for calculating the density of the abrasive is as follows:

$$\rho = \frac{m}{m + m_1 - m_2}\rho_0 \quad (1)$$

where ρ represents the density of abrasives, and ρ_0 denotes the measured density of distilled water at room temperature.

The sintered ceramic corundum abrasives were sieved by selecting 40 abrasive grains of 40–60 mesh. On a diamond static compressive strength tester (ZMC-II; Zhengzhou Institute of Abrasives and Grinding), a single-particle compressive strength test was performed. The average of 40 randomly chosen grains was used to compute the final value for the single-particle compressive strength values for the abrasive samples.

The hardness of abrasives refers to their ability to resist the formation of indentations on the surface under a given pressure [30]. The Vickers hardness of the abrasives used in this investigation was assessed using the indentation method. After polishing, a hardness tester was used to gauge the sintered abrasive block samples' Vickers hardness (HMAS-D10; Shanghai Yanrun Optical Machinery Technology Co., Ltd., Shanghai, China).

Ball milling toughness refers to the capacity of abrasives to resist crushing in the ball grinding process. To measure ball milling toughness, 200 g of dry abrasives at 80 °C were taken for 1 h and then cooled to room temperature. The samples were then screened using standard sample screens of 40 mesh, 60 mesh, and 80 mesh, according to the size of the samples. The samples were placed on the selected top sample screen and screened on a screen machine for 10 min. The total samples retained in the third-layer test screen were then replaced on the selected top-layer test screen for another 10 min. The samples retained on the third layer of the test screen after two screens were removed as tested samples.

Next, 100 g of the retained samples and 1000 g of steel balls were placed into the ball mill tank. The rotation speed was set at 75 r/min, and the total rotation number was 1200 revolutions. After ball milling, the samples were removed, and the material in the

ball mill tank was collected with a brush. The samples were then recovered and weighed as M_1 (accurate to 0.1 g). The samples were sifted using a sieve machine for 5 min, and the samples of the third test screen (80 mesh) were weighed as m_1 (accurate to 0.1 g). This process was repeated for the other sample to obtain data M_2 and m_2.

The toughness value of the tested sample was calculated using Formula (2):

$$\text{ball milling toughness} = \frac{m_1+m_2}{M_1+M_2} \cdot 100\% \quad (2)$$

4. Conclusions

In this study, CaO-TiO_2-SiO_2 was used as an additive system to prepare ceramic corundum abrasives via the sol-gel method. Compared to the samples without additives, the structure of the prepared abrasives was denser, and their single-particle compressive strength and Vickers hardness were significantly improved. The synergy effect of TiO_2, SiO_2, and CaO promoted the sintering process of ceramic corundum abrasives. The morphology of the grains varied with the changes of molar ratio of additives. As the content of SiO_2 and TiO_2 increased, the grains tended to form needle-like/rod-like anisotropic grains. A moderate content of CaO facilitates the formation of equiaxed grains, whereas excessive addition of CaO led to AGG. Equiaxed grains improved the density and Vickers hardness of abrasives, while anisotropic grains increased single-particle compressive strength. Ball milling had a mechanical activation effect, which improved the mixing uniformity and nucleation density, leading to smaller equiaxed grains. However, abrasives with higher compressive strength were prepared without ball milling. Low-cost, high-strength ceramic corundum abrasives have broad application prospects. These findings provide a theoretical basis and practical guidance for the batch preparation of ceramic corundum abrasives. Meanwhile, some important conclusions are as follows:

The samples with the best morphology and performance were obtained when adding CaO-TiO_2-SiO_2 with a molar ratio of 3:4:9. The single-particle compressive strength was 51.45 N, density was 3.94 $g \cdot cm^{-3}$, Vickers hardness was 17.03 GPa, ball milling toughness was 97.4%, and average grain size was 0.98 μm.

The method of additive introduction can also affect the mechanical properties of ceramic corundum abrasives. The performance of the scale method is slightly better than that of the ceramic corundum prepared by the ball grinding method, but it has overall reached a high level, which meets the requirements of practical application.

Author Contributions: All authors have read and agreed to the published version of the manuscript.

Funding: This research received no external funding.

Data Availability Statement: Data are contained in the article.

Acknowledgments: We would like to express our sincere gratitude to the Key Laboratory for Advanced Ceramics and Machining Technology of the Ministry of Education, School of Materials Science and Engineering, Tianjin University, for providing the necessary facilities and support for this research. We also extend our heartfelt thanks to our research group members, colleagues, and teachers for their valuable feedback and insightful discussions, which greatly contributed to the success of this project.

Conflicts of Interest: The authors declare no conflict of interest.

References

1. Filipovic, S.; Obradovic, N.; Markovic, S.; Djordjevic, A.; Balac, I.; Dapcevic, A.; Rogan, J.; Pavlovic, V. Physical properties of sintered alumina doped with different oxides. *Sci. Sinter.* **2018**, *50*, 409–419. [CrossRef]
2. Godino, L.; Pombo, I.; Girardot, J.; Sanchez, J.A.; Iordanoff, I. Modelling the wear evolution of a single alumina abrasive grain: Analyzing the influence of crystalline structure. *J. Mater. Process. Technol.* **2020**, *277*, 116464. [CrossRef]
3. Krell, A.; Blank, P.; Wagner, E.; Bartels, G. Advances in the Grinding Efficiency of Sintered Alumina Abrasives. *J. Am. Ceram. Soc.* **2005**, *79*, 763–769. [CrossRef]

4. Huang, L.; Wang, J.; Zhu, Y.; Li, Z.; Sun, K. Effect of TiO_2–SiO_2 on microstructure and mechanical characteristics of zirconium corundum abrasives by sol-gel method. *J. Alloy. Compd.* **2019**, *802*, 229–234. [CrossRef]
5. Huang, B.; Li, C.; Zhang, Y.; Ding, W.; Yang, M.; Yang, Y.; Zhai, H.; Xu, X.; Wang, D.; Debnath, S.; et al. Advances in fabrication of ceramic corundum abrasives based on sol–gel process. *Chin. J. Aeronaut.* **2020**, *34*, 1–17. [CrossRef]
6. Li, N.; Zhu, Y.-M.; Gao, K.; Li, Z.-H. Preparation of sol-gel derived microcrystalline corundum abrasives with hexagonal platelets. *Int. J. Miner. Met. Mater.* **2013**, *20*, 71–75. [CrossRef]
7. Hashimoto, S.; Horita, S.; Ito, Y.; Hirano, H.; Honda, S.; Iwamoto, Y. Synthesis and mechanical properties of porous alumina from anisotropic alumina particles. *J. Eur. Ceram. Soc.* **2010**, *30*, 635–639. [CrossRef]
8. Li, Z.; Zhang, A.; Li, Z. A novel low temperature synthesis technique of sol-gel derived nanocrystalline alumina abrasive. *J. Sol. Gel Sci. Technol.* **2011**, *57*, 24–30. [CrossRef]
9. Kumagai, M.; Messing, G.L. Enhanced Densification of Boehmite Sol-Gels by α-Alumina Seeding. *J. Am. Ceram. Soc.* **1984**, *67*, c230–c231. [CrossRef]
10. Yamamura, K.; Kobayashi, Y.; Yasuda, Y.; Morita, T. Fabrication of α-alumina by a combination of a hydrothermal process and a seeding technique. *J. Funct. Mater. Lett.* **2018**, *11*, 18500421–18500424. [CrossRef]
11. Bye, G.C.; Simpkin, G.T. Influence of Cr and Fe on Formation of α-Al_2O_3 from γ-Al_2O_3. *J. Am. Ceram. Soc.* **1974**, *57*, 367–371. [CrossRef]
12. McArdle, J.L.; Messing, G.L. Transformation, microstructure development, and densification in alpha Fe_2O_3-seeded boehmite-derived alumina. *J. Am. Ceram. Soc.* **2005**, *76*, 214–222. [CrossRef]
13. Kim, H.S.; Kang, M. Rapid crystal phase transformation into hexagonally shaped α-alumina using AlF_3 seeds. *J. Sol-Gel Sci. Technol.* **2013**, *68*, 110–120. [CrossRef]
14. Riello, D.; Zetterström, C.; Parr, C.; Braulio, M.; Moreira, M.; Gallo, J.; Pandolfelli, V. AlF_3 reaction mechanism and its influence on α-Al_2O_3 mineralization. *Ceram. Int.* **2016**, *42*, 9804–9814. [CrossRef]
15. Karagedov, G.; Myz, A. Preparation and sintering pure nanocrystalline α-alumina powder. *J. Eur. Ceram. Soc.* **2012**, *32*, 219–225. [CrossRef]
16. Lee, S.-H.; Kim, D.-Y.; Hwang, N.M. Effect of anorthite liquid on the abnormal grain growth of alumina. *J. Eur. Ceram. Soc.* **2002**, *22*, 317–321. [CrossRef]
17. Yoshida, H.; Ikuhara, Y.; Sakuma, T. High temperature plastic deformation related to grain boundary chemistry in cation-doped alumina. *Mater. Sci. Eng. A* **2004**, *387*, 723–727. [CrossRef]
18. Riu, D.; Kong, Y.; Kim, H. Effect of Cr_2O_3 addition on microstructural evolution and mechanical properties of Al_2O_3. *J. Eur. Ceram. Soc.* **2000**, *20*, 1475–1481. [CrossRef]
19. Han, Y.; Li, Z.; Zhu, Y. Effect of MgO-TiO_2-SiO_2 additions on in-situ anisotropic grains growth and mechanical properties of corundum abrasive using pseudo-boehmite as raw material. *Ceram. Int.* **2020**, *46*, 1934–1939. [CrossRef]
20. Bae, S.I.; Baik, S. Determination of Critical Concentrations of Silica and/or Calcia for Abnormal Grain Growth in Alumina. *J. Am. Ceram. Soc.* **1993**, *76*, 1065–1067. [CrossRef]
21. Park, C.W.; Yoon, D.Y. Effects of SiO_2, CaO_2, and MgO Additions on the Grain Growth of Alumina. *J. Am. Ceram. Soc.* **2004**, *83*, 2605–2609. [CrossRef]
22. Juhász, A.Z. Aspects of mechanochemical activation in terms of comminution theory. *Colloids Surf. A Physicochem. Eng. Asp.* **1998**, *141*, 449–462. [CrossRef]
23. Jung, J.; Baik, S. Abnormal Grain Growth of Alumina: CaO Effect. *J. Am. Ceram. Soc.* **2003**, *86*, 644–649. [CrossRef]
24. Brydson, R.; Chen, S.-C.; Riley, F.L.; Milne, S.J.; Pan, X.; Rühle, M. Microstructure and Chemistry of Intergranular Glassy Films in Liquid-Phase-Sintered Alumina. *J. Am. Ceram. Soc.* **2005**, *81*, 369–379. [CrossRef]
25. Ahn, J.H.; Lee, J.-H.; Hong, S.-H.; Hwang, N.-M.; Kim, D.-Y. Effect of the Liquid-Forming Additive Content on the Kinetics of Abnormal Grain Growth in Alumina. *J. Am. Ceram. Soc.* **2003**, *86*, 1421–1423. [CrossRef]
26. Altay, A.; Gülgün, M.A. Microstructural Evolution of Calcium-Doped α-Alumina. *J. Am. Ceram. Soc.* **2003**, *86*, 623–629. [CrossRef]
27. Kim, Y.-M.; Hong, S.-H.; Kim, D.-Y. Anisotropic Abnormal Grain Growth in TiO_2/SiO_2-Doped Alumina. *J. Am. Ceram. Soc.* **2004**, *83*, 2809–2812. [CrossRef]
28. You, J.; Yang, T.; Feng, D.; Li, Z. Synthesis and two-step sintering behavior of solution derived corundum abrasives with plate-like grains. *Ceram. Int.* **2018**, *44*, 12615–12620. [CrossRef]
29. Hu, D.; Li, Z.; Zhu, Y. Effect of ZnF_2-TiO_2-SiO_2 additions on the two-step sintering behavior and mechanical properties of sol–gel derived corundum abrasive. *Ceram. Int.* **2016**, *42*, 7373–7379. [CrossRef]
30. Krell, A.; Blank, P. Grain Size Dependence of Hardness in Dense Submicrometer Alumina. *J. Am. Ceram. Soc.* **1995**, *78*, 1118–1120. [CrossRef]